PNAS COMMENTARY

Toward next-generation molecular imaging

Boyd M. Goodson[a] and Eduard Y. Chekmenev[b,1]

The advent of molecular imaging has revolutionized personalized medical care for a wide range of diseases. Positron emission tomography (PET) is the leading clinical molecular imaging modality, enabling whole-body imaging of biochemical processes via radioactive tracers in tissues deep within the body. An ever-expanding palette of PET tracers has been developed over the past few decades to help diagnose, stage, and monitor the response to treatment of various diseases. Indeed, 2 million PET scans are performed in the United States annually. By far, ^{18}F-labeled [^{18}F-]-fluorodeoxyglucose (FDG) is the most widely employed clinical PET tracer. The blockbuster success of FDG-PET relates to its ability to image aberrant cellular glucose uptake, which is up-regulated in many metabolically challenged diseases—including many cancers (1). Importantly, changes in cellular metabolism often occur before significant anatomical changes take place [typically captured by a computed tomography (CT) scan]. As a result of this powerful "glimpse into the future" that such metabolic information can provide, modern cancer care heavily relies on FDG-PET molecular imaging to stage cancer patients and monitor their treatment response (1). Despite the high cost of an FDG-PET scan (several thousand USD), it provides valuable information regarding treatment efficacy, allowing doctors to discontinue treatments that may be ineffective or even detrimental—as well as cost orders of magnitude more than the scan itself. In the United States, the medical treatment costs for cancer alone approach $200 billion per year (2), not counting an additional annual cost of $150 billion in lost productivity to the US economy (3).

Despite the transformational impact of FDG-PET on cancer care, this lifesaving exam has several notable disadvantages. First, it employs ionizing radiation, derived both from the injected FDG itself and from accompanying anatomical CT scans; therefore, whole-body PET-CT scanning comes with a cancer risk (4), and these examinations must be clinically justified. This limitation is exacerbated by the requirement that a baseline scan be performed before a cancer patient begins a given treatment regimen. In practice, the scan may need to be repeated, multiple times per year in some cases. Second, the FDG-PET exam is time-consuming, often requiring the patient to fast for several hours before the exam—with approximately 1 h for the tracer uptake and clearance from the surrounding tissues, and with the scan itself taking half an hour. Third, the compounding effect of the above limitations makes it challenging to perform frequent follow-up FDG scans or perform molecular imaging scans with other ^{18}F-labeled tracers—despite the fact that information gained about other molecular pathways could further improve treatment outcomes. Fourth, FDG administration often yields a strong PET background signal in many organs at the time of the scan (most notably in the brain, heart, and prostate) making it practically unusable in these organs for the associated diseases.

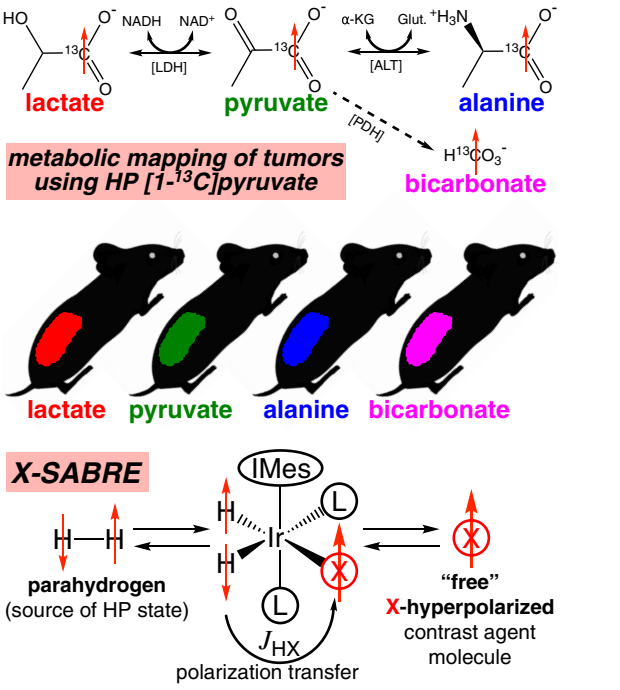

Fig. 1. The concept of metabolic imaging using HP MRI contrast agents and a schematic of SABRE hyperpolarization. Metabolic mapping of injected HP [1-^{13}C]pyruvate and downstream metabolites enables imaging of aberrant metabolic fluxes in cancer and other metabolically challenged diseases. Simultaneous chemical exchange of parahydrogen (the source of NMR hyperpolarization) and a to-be-HP substrate (i.e., a contrast agent molecule) with a metal center results in hyperpolarization of "free" contrast agent molecules in solution over multiple exchange cycles.

A next-generation molecular imaging technology is being developed to address the limitations of FDG-PET exams. In PNAS, Lindale et al. (5) present a major breakthrough in the development of this new clinical technology. The new molecular imaging technology employs MRI scans, which do not expose patients to ionizing radiation. Before continuing, it is important to note that the sensitivity of conventional MRI is

Author affiliations: [a]School of Chemical & Biomolecular Sciences and Materials Technology Center, Southern Illinois University, Carbondale, IL 62901; and [b]Department of Chemistry, Integrative Biosciences, Karmanos Cancer Institute, Wayne State University, Detroit, MI 48202

Author contributions: B.M.G. and E.Y.C. wrote the paper.

Competing interest statement: B.M.G. and E.Y.C. declare a stake of ownership in XeUS Technologies, Ltd. E.Y.C. holds stock of Vizma Life Sciences (VLS) and serves on the Scientific Advisory Board (SAB) of VLS. B.M.G. and E.Y.C. have multiple pending and awarded patents in the area of NMR hyperpolarization.

Copyright © 2024 the Author(s). Published by PNAS. This article is distributed under Creative Commons Attribution-NonCommercial-NoDerivatives License 4.0 (CC BY-NC-ND).

See companion article, "Multi-axis fields boost SABRE hyperpolarization," 10.1073/pnas.2400066121.

[1]To whom correspondence may be addressed. Email: chekmenevlab@gmail.com.

Published April 24, 2024.

Downloaded from https://www.pnas.org by "SOUTHERN ILLINOIS UNIVERSITY, MORRIS LIBRARY/PERIODICALS" on April 24, 2024 from IP address 131.230.80.96.

normally too low to track metabolic transformations in vivo: MRI works by detecting the magnetic response of nuclear spins and usually the degree of alignment (called polarization) of nuclear spins is minuscule—even within the strong magnet of an MRI scanner. Thus, the anatomical images from most MRI scans are actually provided by species whose concentrations are high enough to outweigh that low polarization (i.e., the body's water and fat). However, one can exploit "tricks" from quantum physics to transiently increase the nuclear spin polarization (*P*) far from its normal equilibrium value, a process dubbed hyperpolarization. Indeed, several hyperpolarization techniques have been developed that can increase *P* by 4 to 6 orders of magnitude, resulting in correspondingly massive gains in MRI detection sensitivity (6, 7). As a result, it has now become possible to image low-concentration molecules in deep tissue. Indeed, hyperpolarized (HP) ^{129}Xe gas, which can be inhaled and used for lung imaging, recently became the first FDA-approved HP MRI contrast agent. Moreover, HP [1-^{13}C]pyruvate is now under evaluation in over 50 clinical trials according to clinicaltrials.gov.

In PNAS, Lindale et al. greatly expand our knowledge of how polarization can be efficiently transferred from parahydrogen-derived hydrides to the spins of X-nuclei (typically ^{13}C or ^{15}N nuclei) within the exchangeable substrate molecules—a process dubbed X-SABRE.

When injected, HP [1-^{13}C]pyruvate is rapidly metabolized into HP [1-^{13}C]lactate, [1-^{13}C]alanine, and [^{13}C]bicarbonate via several metabolic pathways (8, 9). The injected HP [1-^{13}C]pyruvate and the produced HP metabolites can be distinguished from one another by their different frequencies and separately imaged, allowing maps of each HP substance to be created (Fig. 1). In so doing, one can also obtain the metabolic fluxes of each substance within a given tissue in real time, as opposed to the more limited information regarding tracer uptake provided by FDG-PET (8, 9). It has been shown that an HP [1-^{13}C]pyruvate MRI scan can probe the response to cancer treatment similarly to an FDG-PET scan (10). Moreover, as a result of the described technology advantages, a HP MRI molecular imaging scan can be performed in only about a minute—even in the presence of background HP [1-^{13}C]pyruvate signals from the surrounding tissues.

For clinical studies (11, 12), HP [1-^{13}C]pyruvate is currently produced via a technique called dissolution dynamic nuclear polarization (d-DNP). d-DNP has proven to be a powerful and general hyperpolarization technology for a wide range of prospective biomedical applications, enabling amazing progress to date (8). However, d-DNP technology is slow (requiring roughly an hour to produce HP [1-^{13}C]pyruvate), suffers from low throughput and high cost (the hyperpolarizer device alone can cost $2M) and has complex siting requirements due to the reliance on high-field superconducting magnets and cryogenic temperatures (11, 12). Thus, alternative hyperpolarization technologies are being actively pursued to enable efficient, low-cost production of HP [1-^{13}C]pyruvate and other HP molecular imaging probes (13). One such technology is signal amplification by reversible exchange (SABRE), which relies on simultaneous chemical exchange of parahydrogen—a "spin isomer" of ordinary molecular hydrogen (H_2) gas—and to-be-HP molecules with a metal-based ligating catalyst (14). The pure spin order of parahydrogen acts as a reservoir of hyperpolarization, which can be spontaneously transferred to the nuclear spins of the to-be-HP molecules via spin–spin couplings established during the transient formation of the SABRE-active complex (Fig. 1). Following polarization, the exchangeable HP substrate is then released into the solution phase. Multiple cycles of the SABRE process subsequently lead to the accumulation of bulk hyperpolarization in the free substrate molecules in solution—usually in under a minute.

In PNAS, Lindale et al. (5) greatly expand our knowledge of how polarization can be efficiently transferred from parahydrogen-derived hydrides to the spins of X-nuclei (typically ^{13}C or ^{15}N nuclei) within the exchangeable substrate molecules—a process dubbed X-SABRE. Unlike hydrogen nuclei (^{1}H), ^{13}C and ^{15}N nuclei can retain the HP state for minutes in vivo, which is sufficiently long to probe metabolic fluxes. Thus, X-SABRE hyperpolarization of ^{13}C and ^{15}N nuclear spins in biocompatible molecules has been a highly active area of research (15, 16). The X-SABRE process is most efficient in ultraweak microtesla magnetic fields (i.e., a field that is much less than even the Earth's field) (15, 16), where the energetics of parahydrogen and "X" spin flips can be properly matched, and both static and alternating fields can be readily controlled in multiple spatial directions. However, the X-SABRE polarization process can be surprisingly complex, as the *P* evolution reflects a sensitive interplay of the underlying spin dynamics and the rapid chemical exchange of the various species involved. Lindale et al. employ a novel evolutionary strategy algorithm for numerical optimization of X-SABRE hyperpolarization processes (5). Specifically, Lindale et al. have developed an approach called multi-axis computer-aided heteronuclear transfer enhancement for SABRE, or MACHETE-SABRE (5). Despite the fact that the computer-aided MACHETE-SABRE pulse sequences are far from intuitive in their design, they result in substantially more efficient hyperpolarization of the targeted X-nuclei. Indeed, Lindale et al. demonstrate that the efficiency of X-SABRE hyperpolarization can be improved by as much as sevenfold using the new MACHETE-SABRE approach, compared to that attained using a static microtesla field alone (5). This finding is important because the degree of polarization of the X-nucleus is a critical factor determining the successful utilization of HP [1-^{13}C]pyruvate and other metabolic HP probes in vivo: The resolution and the quality of the metabolic mapping scan is directly proportional to the ^{13}C polarization (P_{13C}). Thus, to increase the HP signal readout, one has to maximize P_{13C}—ideally to the order of unity. The MACHETE-SABRE approach demonstrated by Lindale at al. thus addresses a critical translational challenge of SABRE technology for production of HP [1-^{13}C]pyruvate contrast agent, as well as for other emerging molecular imaging probes (17).

The SABRE process is remarkably fast and simple in terms of experimental requirements. Indeed, HP solutions of [1-^{13}C]pyruvate are produced near room temperature in

Downloaded from https://www.pnas.org by "SOUTHERN ILLINOIS UNIVERSITY, MORRIS LIBRARY/PERIODICALS" on April 24, 2024 from IP address 131.230.80.96.

only a minute, using hardware components costing less than $10,000 (18–20). The utility of SABRE hyperpolarization for production and in vivo molecular imaging of HP [1-^{13}C] pyruvate has been recently demonstrated (21, 22), thus potentially making SABRE a game-changing technology for enabling next-generation MRI-based molecular imaging modalities. The ongoing research and commercialization work in this rapidly expanding field aims to develop clinical production of HP [1-^{13}C]pyruvate and other emerging molecular probes, thereby providing robust, inexpensive, and scalable access to HP agents for a wide range of stake holders—ranging from scientists, to doctors, and patients. All in all, SABRE hyperpolarization technology has the potential to revolutionize molecular imaging and treatment of a wide range of metabolically challenged diseases, most notably including cancer, diabetes, and various neurodegenerative disorders.

ACKNOWLEDGMENTS. B.M.G. and E.Y.C.'s research is supported by the NIH (R21 EB033872, R21 HL154032, and R01 EB034197), DOD (CDMRP W81XWH-20-10576 and W81XWH-20-10578), and NSF (CHE-1905341, CHE-2303622, and CHE-1904780).

1. J. W. Fletcher *et al.*, Recommendations on the use of ^{18}F-FDG PET in oncology. *J. Nucl. Med.* **49**, 480–508 (2008).
2. NCI, Financial burden of cancer care (2023). https://progressreport.cancer.gov/after/economic_burden. Accessed 24 March 2024.
3. C. J. Bradley *et al.*, Productivity costs of cancer mortality in the United States: 2000–2020. *J. Natl. Cancer Inst.* **100**, 1763–1770 (2008).
4. B. Huang, M.W.-M. Law, P.-L. Khong, Whole-body PET/CT scanning: Estimation of radiation dose and cancer risk. *Radiology* **251**, 166–174 (2009).
5. J. R. Lindale *et al.*, Multi-axis fields boost SABRE hyperpolarization. *Proc. Natl. Acad. Sci. U.S.A.* **121**, e2400066121 (2024).
6. P. Nikolaou, B. M. Goodson, E. Y. Chekmenev, NMR hyperpolarization techniques for biomedicine. *Chem. Eur. J.* **21**, 3156–3166 (2015).
7. J. Eills *et al.*, Spin hyperpolarization in modern magnetic resonance. *Chem. Rev.* **123**, 1417–1551 (2023).
8. J. Kurhanewicz *et al.*, Hyperpolarized ^{13}C MRI: Path to clinical translation in oncology. *Neoplasia* **21**, 1–16 (2019).
9. F. A. Gallagher *et al.*, Imaging breast cancer using hyperpolarized carbon-13 MRI. *Proc. Natl. Acad. Sci. U.S.A.* **117**, 2092–2098 (2020).
10. S. E. Day *et al.*, Detecting tumor response to treatment using hyperpolarized C-13 magnetic resonance imaging and spectroscopy. *Nat. Med.* **13**, 1382–1387 (2007).
11. J. H. Ardenkjaer-Larsen *et al.*, Dynamic nuclear polarization polarizer for sterile use intent. *NMR Biomed.* **24**, 927–932 (2011).
12. J. H. Ardenkjaer-Larsen *et al.*, Increase in signal-to-noise ratio of > 10,000 times in liquid-state NMR. *Proc. Natl. Acad. Sci. U.S.A.* **100**, 10158–10163 (2003).
13. K. V. Kovtunov *et al.*, Hyperpolarized NMR: d-DNP, PHIP, and SABRE. *Chem. Asian J.* **13**, 1857–1871 (2018).
14. R. W. Adams *et al.*, Reversible interactions with para-hydrogen enhance NMR sensitivity by polarization transfer. *Science* **323**, 1708–1711 (2009).
15. T. Theis, M. Truong, A. M. Coffey, E. Y. Chekmenev, W. S. Warren, LIGHT-SABRE enables efficient in-magnet catalytic hyperpolarization. *J. Magn. Reson.* **248**, 23–26 (2014).
16. T. Theis *et al.*, Microtesla SABRE enables 10% nitrogen-15 nuclear spin polarization. *J. Am. Chem. Soc.* **137**, 1404–1407 (2015).
17. O. G. Salnikov, D. B. Burueva, I. V. Skovpin, I. V. Koptyug, Parahydrogen-based NMR signal amplification by reversible exchange (SABRE): Recent advances and applications. *Mendeleev Commun.* **33**, 583–596 (2023).
18. S. Nantogma *et al.*, MATRESHCA: Microtesla apparatus for transfer of resonance enhancement of spin hyperpolarization via chemical-exchange and addition. *Anal. Chem.* **96**, 4171–4179 (2024).
19. P. TomHon *et al.*, Temperature cycling enables efficient ^{13}C SABRE-SHEATH hyperpolarization and imaging of [1-^{13}C]-pyruvate. *J. Am. Chem. Soc.* **144**, 282–287 (2022).
20. W. Iali *et al.*, Hyperpolarising pyruvate through signal amplification by reversible exchange (SABRE). *Angew. Chem. Int. Ed.* **58**, 10271–10275 (2019).
21. K. MacCulloch *et al.*, Facile hyperpolarization chemistry for molecular imaging and metabolic tracking of [1-^{13}C]pyruvate in vivo. *J. Magn. Reson. Open* **16**, 100129 (2023).
22. H. de Maissin *et al.*, In vivo metabolic imaging of [1-^{13}C]pyruvate-d3 hyperpolarized by reversible exchange with parahydrogen. *Angew. Chem. Int. Ed.* **62**, e202306654 (2023).

Downloaded from https://www.pnas.org by "SOUTHERN ILLINOIS UNIVERSITY, MORRIS LIBRARY/PERIODICALS" on April 24, 2024 from IP address 131.230.80.96.